Protein dynamics and spectroscopy for ferryl intermediate of Cytochrome *c* Oxidase: A molecular dynamics approach

Vangelis Daskalakis [*†], Stavros C. Farantos [*†] and Constantinos Varotsis [*]

[*]*Department of Chemistry, University of Crete, POBox 2208, 71305, Voutes-Heraklion, Crete, Greece*
[†]*Foundation for Research and Technology-Hellas (FORTH), POBox 1385, 71110, Voutes- Heraklion, Crete, Greece*

Abstract. Cytochrome *c* oxidase is the membrane bound terminal enzyme in the respiratory chain. Molecular oxygen is reduced to water in its heme Fe/Cu_B active site. The O–O bond cleavage produces the ferryl-oxo (Fe^{IV}=O) intermediate. Molecular Dynamics calculations for a part of the protein containing over 8600 atoms are employed to probe the frequencies of vibrational modes which involve the stretching of Fe-O during protonation/deprotonation events near the active site. The role of protein frame for the spectroscopic properties of the ferryl intermediate is proved to be significant, as the intensity of the oxygen sensitive bands is controlled by conformational changes. In addition, the mechanism of the release of the produced water molecules is examined by changing the protonation state of a residue in the entrance of a proton pathway in the enzyme.

Keywords: Cytochrome *c* oxidase, ferryl intermediate, molecular dynamics, Fourier transforms, protein frame.
PACS: 87.15.He

INTRODUCTION

Cytochrome *c* oxidase (CcO) couples the four electron reduction of dioxygen to water with the pump of four protons across the inner mitochondrial membrane attributing to the electrochemical gradient that is used to synthesize ATP. Electrons from *cyt. c* pass through a heme *a* group and are then transferred to the binuclear heme a_3/Cu_B active site (**Fig. 1a**) where dioxygen is reduced. The understanding of the mechanism of action of CcO has been a matter of considerable debate.

In the reaction of the enzyme with O_2 the O-O bond is cleaved producing the ferryl-oxo (Fe^{IV}=O) species (1). The $\mathbf{P_M}$ intermediate (607nm, originating from the MV[1] form of the enzyme) exhibits a ν(Fe-O) at 804 cm^{-1} probed by Resonance Raman spectroscopy. In the reaction of the fully reduced enzyme with O_2 either two peaks are identified in the spectra exhibiting ferryl-oxo character with ν(Fe-O) at 790 and 804 cm^{-1} (shifting to 750 and 764 cm^{-1} with ^{18}O respectively) (2-3) or only the latter (4). It is clear that establishing the dynamics of the protein environment adjacent to the active site subsequent to O-O bond cleavage is first essential in understanding the linkage of oxygen activation with proton translocation and second in assigning the 790/ 804 cm^{-1} peaks.

A proton pathway, called Q, with highly conserved residues, originates at the cytoplasmic side of the membrane and leads through the axial heme a_3 ligand His-411 to the propionate of the heme a_3 pyrrol ring A, and then via Asp-399 (aa_3 *P. denitrificans* numbering) to an accumulation of water molecules (*water pool*). Based on a proposed model (5) on the role of the ring A heme a_3 propionate-Asp-399-H_2O site as a proton carrier to the *water pool* connecting the catalytic binuclear center and the exit/output proton channel, four different protonation cases are possible for the propionate-Asp399 pair (**Fig. 1b**). In addition, Glu278 residue in the entrance of the so-called D-proton pathway seems to play a significant role as a switch coupled to the ability of a proton to propagate along this path (6) or to local structural changes in the region of propionates (7-10).

In this work we study the dynamics of the protein matrix near the active site at the ferryl-oxo oxidation level concentrating on the ν(Fe-O) and the role of Glu278, using Molecular Dynamics (MD) simulations. A model system for the active site with 95 atoms is employed to study in detail the role of anharmonicity on the vibrational modes at several energies.

[1] In the Mixed Valence (MV) form heme a_3 iron /Cu_B active site is reduced, while heme *a* and dinuclear Cu_A sites are oxidized.

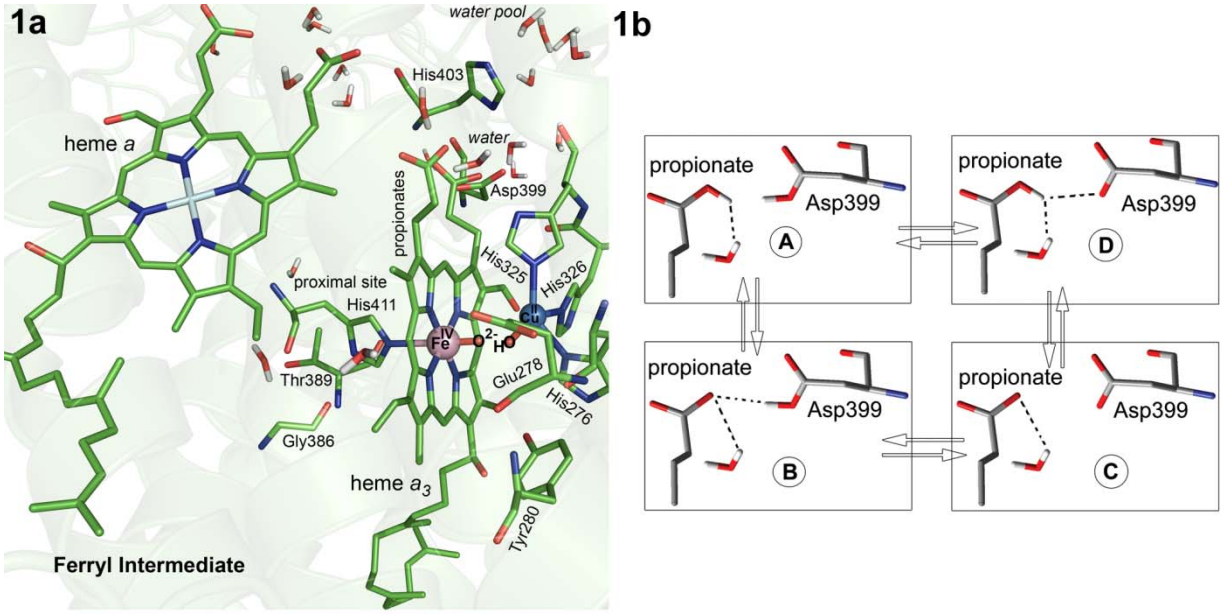

FIGURE 1. (a) Crystal structure of the aa_3 cytochrome *c* oxidase from *P. denitrificans*. *Heme* a_3-Fe/Cu_B active site as well as the *heme a* metal site are shown. In the proximal area amino acids Gly386 and Thr389 are in close proximity to the His411 which coordinates to *heme* a_3 Fe. **(b)** Different protonation states of the propionate-Asp399 pair. In structures A and C all carboxyl groups in equilibrium are protonated or deprotonated respectively, while in B or D structures only one H^+ is available protonating either Asp399 or propionate respectively. Carbon appears grey, oxygen red, nitrogen blue and white is used for hydrogen.

MATERIALS AND METHODS

Molecular Dynamics simulations were carried out with initial cartesian coordinates from the two-subunit aa_3 crystal structure of *P. denitrificans* (PDB code 1AR1). Only the first subunit is used in our simulations with ~8600 atoms in the A, B, C and D cases shown in **Fig. 1b**. Partial charges for the heme *a*/ heme a_3/Cu_B metal sites were derived from DFT optimized models (b3lyp/6-311g* level). An -OH ligand was modeled bound to Cu_B, with heme a_3 iron in the 6-coordinate Fe(IV)=O state. All crystallographic water molecules were retained in the structure (TIP3P force field). Simulations were performed at constant temperature (300K) and a 0.15fs time step for the integrations of equations of motion was used. The software package Tinker 4.2 (11) was employed with the Amber99 force field. Several parameters, especially for the heme groups, were fitted either to DFT data or taken from Charmm27 force field. The bondtype parameter was set to Morse. All amino acids were free to move during the simulations, except one case where a force constant of 7 kcal/mol $Å^2$ was applied to restrain the distance between the C_γ atom of E278 and the Δ-methyl carbon of heme a_3 at its crystallographic value (10). For non-bonded interactions a cutoff distance of 12Å with a smoothing window between 9.6-12Å was applied. Structures were minimized and equilibrated at constant temperature before each simulation. MD simulations and non-linear mechanical analysis (12) were also performed on a model of heme a_3/ Cu_B active site (95 atoms), with the same force field discussed above and without the protein matrix in Fe(IV)=O oxidation level.

RESULTS AND DISCUSSION

The role of protein frame

For the smaller model of 95 atoms three major bands are identified in the derived spectra by Fast Fourier Transforming (FFT) the recorded Fe-O time-distance series (blue line **Fig. 2a**/ 300K, 2.5 ns). Constraining the Fe-His411 distance to its crystallographic value, the 773 cm^{-1} band disappears, while constraining the Fe-O distance the band with peak at 775 cm^{-1} is the dominant one (**Fig. 2b**), allowing us to assign the 773 peak to a bending motion of histidine's imidazole at the proximal region. In **Fig. 2a** the isotopic effect on the ν(Fe-O) spectrum at 300K is depicted. The ^{16}O spectrum exhibits peaks with higher intensities at 773, 810 and 840 cm^{-1}, with the 810 dominating. All

bands are shifted to lower energies by ^{18}O isotopic substitution at the same temperature. 773 cm^{-1} band shifts to 767 cm^{-1} region as this is not a pure Fe-O vibration and should not exhibit a pronounced isotopic effect. We believe that the active site model with only 95 atoms is a reliable system to reproduce the local dynamics and the ν(Fe-O) bands in the spectra of the protein. Work is in progress for studying the anharmonic behavior and localization phenomena in the vibrational modes of the active center which involve Fe-O stretches.

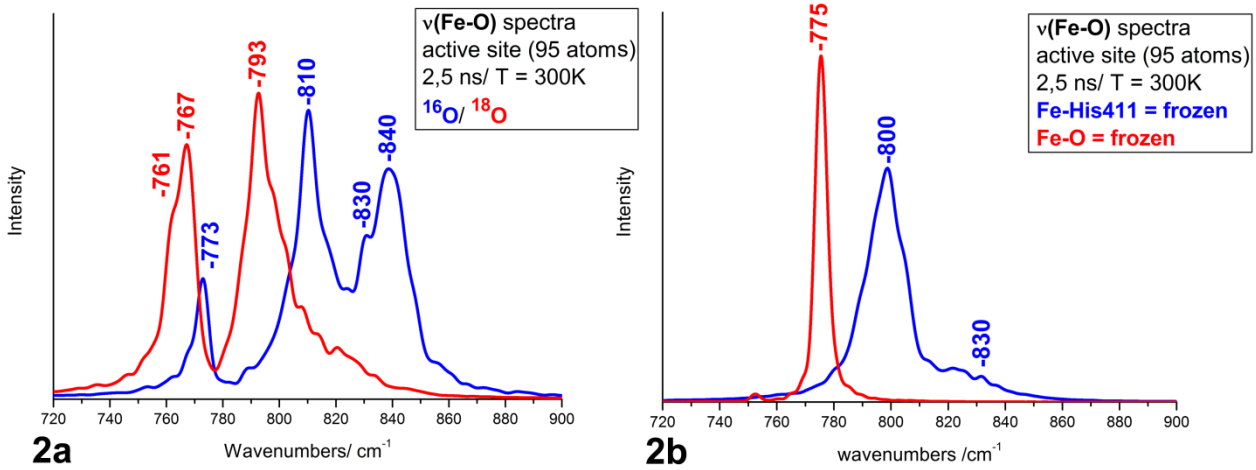

FIGURE 2. Calculated ν(Fe-O) spectra for the active site only (95 atoms) at 300K. (a) $^{16}O/^{18}O$ isotopic effect. (b) When the heme iron axial ligand, histidine 411, is at constant distance from iron, 773 cm^{-1} band disappears (blue line), while it's enhanced when Fe-O distance is frozen (red line).

The ν(Fe-O) spectra (~8600 atoms/ 300K, 0.6 ns) are shown in **Fig. 3**. We observe several peaks for the Fe-O stretching vibrational frequencies the intensities of which heavily depend on the protein frame, as confirmed by overlapping the spectra of different protonated species A, B, C and D. Only minimal shifts are observed for the bands. If the Fe-His411 distance or the Thr389-His411/ Gly386-His411 distances are kept constant, only one oxygen sensitive peak with high intensity appears (data not shown).

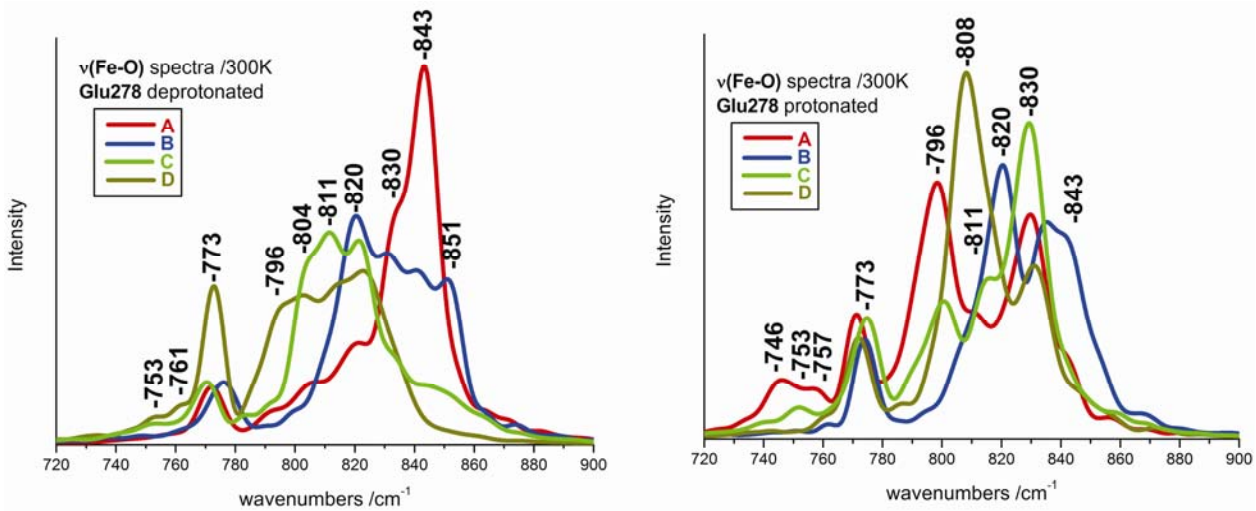

FIGURE 3. Calculated ν(Fe-O) spectra for the different A, B, C and D cases when Glu278 is deprotonated (left group) or protonated (right group). Conformational changes in the protein matrix due to protonation/ deprotonation events seem to strongly influence the intensities of the peaks.

Conformational changes in the proximal region induced by the A, B, C or D cases would alter the hydrogen bonding network in the area and in turn the charge-charge interactions in MD simulations which are proved to be significant for the ν(Fe-O) spectra.

The propionate-Asp399-water equilibrium

We are currently investigating the role of protonation/ deprotonation events of Glu278 to the mobility of H_2O through possible water channels in the propionate-Asp399-H_2O site (6-10). In **Fig. 4** we depict the distance of a water molecule from a propionate group of the heme. Preliminary results indicate that, for protonated Glu278, the water molecule tends to stay for longer times in the region of the propionate-Asp399 site or in the *water pool*. At present, we are studying more trajectories to solidify these results by exploiting the computer power of the European Grid (EGEE).

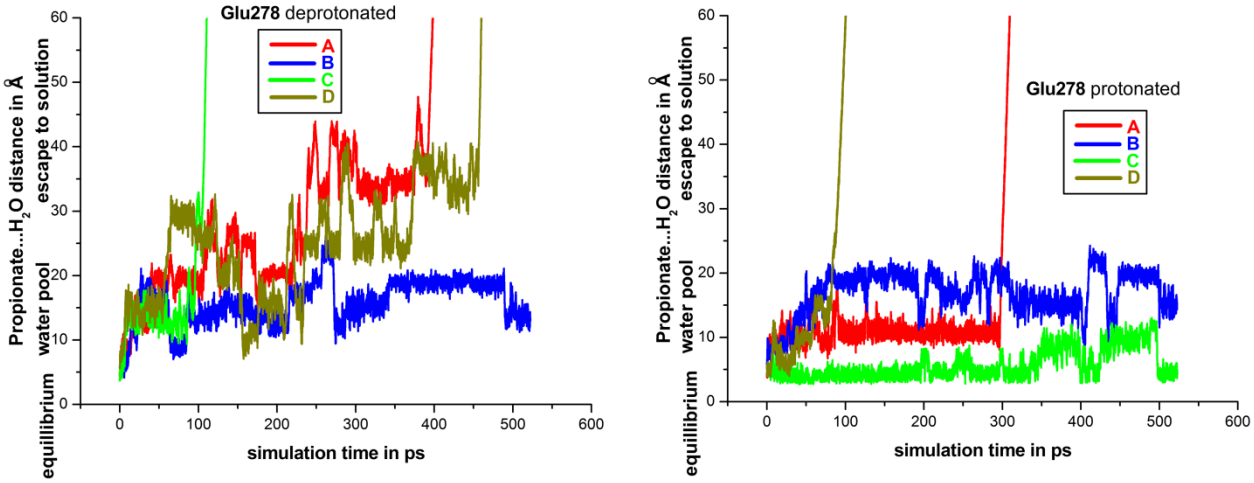

FIGURE 4. Time evolution of the distance between propionate and the water molecule starting with a water molecule in the region of propionate-Asp399. Trajectories represent the fate of the water molecule with time for the four different protonated species A, B, C, and D. We assume that the water molecule remains in the region of propionate-Asp399 when its distance from the pair is less than 5 Å, water is released to *water pool* when the distance is in the range 5-20 Å and it escapes to solution for distances greater than 20 Å.

ACKNOWLEDGMENTS

This research is financially supported by an EU ToK grant (No. MTKD-CT-2005-029583). We are grateful to Manos Giatromanolakis from the Computer Center of FORTH for his assistance in using the European Grid.

REFERENCES

1. C. Varotsis, Y. Zhang, E. H. Appelman and G. T. Babcock, *Proc. Natl. Acad. Sci.* **90**, 237-241 (1993)
2. C. Varotsis and G. T. Babcock, *Biochemistry* **29**, 7357-7362 (1990)
3. T. Ogura, S. Hirota, D. A. Proshlyakov, K. Shinzawa-Itoh, S. Yoshikawa and T. Kitagawa, *J. Am. Chem. Soc.* **118**, 5443-5449 (1996)
4. S. Han, S. Takahashi and D. L. Rousseau, *J. Biol. Chem.* **275**, 1910-1919 (2000)
5. K. Koutsoupakis, T. Soulimane and C. Varotsis, *Biophys. J.* **86**, 2438-2444 (2004)
6. J. Xu and G. A. Voth, *Proc. Natl. Acad. Sci. U.S.A.* **102**, 6795-6800 (2005)
7. M. Svensson-Ek, J. Abramson, G. Larsson, S. Tornröth, P. Brzezinski and S. Iwata, *J. Mol. Biol.* **321**, 329–339 (2002).
8. S. A. Seibold, D. A. Mills, S. Ferguson-Miller and R. I. Cukier, *Biochemistry* **44**, 10475–10485 (2005).
9. M. Lübben, A. Prutsch, B. Mamat and K. Gerwert, *Biochemistry* **38**, 2048–2056 (1999).
10. M. Wikström, C. Ribacka, M. Molin, L. Laakkonen, M. Verkhovsky and A. Puustinen, *Proc. Natl. Acad. Sci. USA* **102**, 10478–10481 (2005).
11. J. W. Ponder (2004) *Tinker 4.2*, Washington University.
12. S. C. Farantos, *J. Chem. Phys.* **126**, 175101-175107 (2007)